catalysts

MDPI

Article

Exploring the Effect of Au/Pt Ratio on Glycerol Oxidation in Presence and Absence of a Base

Alberto Villa [1,*], Andrea Jouve [1], Felipe J. Sanchez Trujillo [2], Davide Motta [2], Laura Prati [1] and Nikolaos Dimitratos [2,*]

[1] Dipartimento di Chimica, Università degli Studi di Milano, via Golgi 19, I-20133 Milano, Italy; Andrea.Jouve@unimi.it (A.J.); Laura.Prati@unimi.it (L.P.)

[2] Cardiff Catalysis Institute, School of Chemistry, Cardiff University, Main Building, Park Place, Cardiff CF10 3AT, UK; SanchezF@cardiff.ac.uk (F.J.S.T.); MottaD@cardiff.ac.uk (D.M.)

* Correspondence: Alberto.Villa@unimi.it (A.V.); DimitratosN@Cardiff.ac.uk (N.D.); Tel.: +39-0250314361 (A.V.); +44-(0)2920874082 (N.D.)

Received: 24 December 2017; Accepted: 29 January 2018; Published: 31 January 2018

Abstract: Bimetallic AuPt nanoparticles with different Au:Pt ratios (molar ratio: 9-1, 8-2, 6-4, 2-8, 1-9) and the corresponding Au and Pt monometallic ones were prepared by sol immobilization and immobilized on commercial TiO_2 (P25). The catalytic activity was evaluated in the liquid phase glycerol oxidation in presence and absence of a base (NaOH). It was found that the Au:Pt molar ratio and reaction conditions strongly influence the catalytic performance. In the presence of NaOH, Au-rich catalysts were more active than Pt-rich ones, with the highest activity observed for Au_9Pt_1/TiO_2 (6575 h^{-1}). In absence of a base, a higher content of Pt is needed to produce the most active catalyst (Au_6Pt_4/TiO_2, 301 h^{-1}). In terms of selectivity, in presence of NaOH, Au-rich catalysts showed a high selectivity to C3 products (63–72%) whereas Pt-rich catalysts promote the formation of formic and glycolic acids. The opposite trend was observed in absence of a base with Pt-rich catalysts showing higher selectivity to C3 products (83–88%).

Keywords: gold-platinum; glycerol oxidation; base; base free

1. Introduction

Biomass is a valid renewable alternative to fossil fuels for the production of valuable fine chemicals and fuels [1,2]. One of the main alternative bio-renewable materials is triglycerides, which are the major component of vegetable oils, waste grease, and oil-processing waste [1,2]. The materials have been utilized for the production of biodiesel by the transesterification of triglycerides with methanol, with glycerol as the main by-product. It is expected that substantial amounts of crude glycerol will have to be processed as waste with the current worldwide annual production of biodiesel being around 30 million tons. Therefore, the large amount of glycerol generated is a potential environmental problem, since it cannot be disposed of in the environment. Due to the fact that glycerol is a highly functionalized molecule, it can be utilized as a platform chemical for the production of high-added-value products [3,4]. Glycerol can be converted through oxidation processes to a variety of valuable chemicals, such as dihydroxyacetone, glyceraldehyde, glyceric acid, glycolic acid, tartronic acid, hydroxypyruvic acid, and lactic acid [3,4]. Different supported noble metal nanoparticles (Au, Pd, Pt, Ru) have been used as catalysts for this reaction with molecular oxygen as oxidant. Pt and Pd catalysts were the first to show a good activity in this reaction [5,6]. However, a drawback in using these catalysts is the deactivation due to metal overoxidation and irreversible adsorption of products and intermediates [5,6]. On the contrary, gold has been demonstrated to be active, selective and a long-life catalyst [7]. The main limitation of gold monometallic catalysts appears to be the requirement for basic conditions to promote the first step of the oxidative dehydrogenation (H-abstraction) [8,9].

Different groups have demonstrated that combining Au to Pd or Pt, is advantageous in terms of activity/selectivity and durability of the catalyst, overcoming the limitation of the corresponding monometallic catalysts [10–15]. For example, we have shown that alloying Au to Pd leads to an enhancement in the activity and selectivity to glyceric acid compared to monometallic Au and Pd [10]. Moreover using bimetallic systems, the deactivation of the catalysts on reuse was significantly diminished. The effect of the molar ratio of Au/Pd in supported carbon bimetallic Au−Pd catalysts in terms of activity and product distribution, was investigated. In particular it was shown that Au-rich catalysts are more active than Pd-rich ones; on the contrary, these latter ones are more selective to glyceric acid [16,17]. As a consequence of using basic conditions, salts of acids are obtained instead of free carboxylic acids, making purification a challenge and limiting their industrial usefulness. In the last years, different groups demonstrated that by alloying Au with Pt it is possible to obtain an effective catalytic system for glycerol oxidation, in terms of activity and selectivity even in the absence of a base [18–20]. The support can strongly influence activity and selectivity of the AuPt system in glycerol oxidation. For example, we have shown that at 80 °C, basic supports (MgO, NiO) promoted the activity but also increased C-C bond cleavage reactions, whereas acidic supports (MCM41, SiO_2, H-mordenite and sulfated-ZrO_2) showed a higher selectivity (>80%) to C3 oxidation products, glyceric acid and glyceraldehyde) [21]. However, decreasing the temperature to 25 °C, also AuPt nanoparticles supported on MgO and hydrotalcite (HT) convert glycerol to glyceric acid with good selectivity (73–78%) [19]. Few studies presented an investigation on the effect of Au-Pt atomic ratio in base free glycerol oxidation, showing that Pt-rich systems are more active than Au-rich ones [22–25]. For example, Tongsakul et al. demonstrated that $Pt_{60}Au_{40}$/HT was the most active and selective to glyceric acid (78% of selectivity at 73% of conversion) [22], whereas Yang et al. reported a selectivity of 60.4% to glyceric acid and 25.7% to glyceraldehyde at 60.4% of conversion using $Pt_{70}Au_{10}$/graphene-oxide [23]. However, most of these systems seem to suffer from deactivation after prolonged reuses, probably due to leaching into the solution of the active phase or irreversible adsorption of the diacid products. We recently showed that AuPt nanoparticles supported on commercial TiO_2 P25 are active and durable systems for both oxidation and hydrogenolysis of polyols [26,27].

In the present work, commercial TiO_2 (P25) was used as the selected support for Au_xPt_y bimetallic systems with different Au-Pt ratio (molar ratio: 9-1, 8-2, 6-4, 2-8, 1-9) and the corresponding monometallic catalysts. The catalysts have been tested in the liquid-phase oxidation of glycerol either in the presence or absence of a base. The aim of this paper is to investigate Pt- and Au-rich catalysts at two different pH conditions, keeping in mind the different mechanism of reaction of the two metals under acidic or basic conditions. The stability of the catalysts has been also investigated.

2. Results

Au_xPt_y/TiO_2 bimetallic catalysts with different Au:Pt atomic ratios, and the corresponding Au and Pt monometallic ones were prepared by the sol immobilization method using polyvinyl alcohol (PVA) as protective agent, following an experimental procedure reported by our group [26,27]. The morphology of the catalysts was investigated by means of transmission electron microscopy (TEM) and X-ray photoelectron spectroscopy (XPS). The characterization of Au/TiO_2 and Pt/TiO_2 was reported in previous studies showing an average metal particle size of 3.5 and 3.6 nm, respectively [26]. The mean particle diameter and the particle distribution of the Au_xPt_y bimetallic systems are reported in Figure 1. TEM images revealed a good dispersion of Au_xPt_y nanoparticles on the surface of TiO_2 and a similar mean particle size (2.9–3.3 nm) with a particle size distribution of 1.0–6.0 nm for all the series of bimetallic catalysts. A detailed HRTEM characterization of the bimetallic Au_6Pt_4/TiO_2 catalysts has been previously reported by C. E. Chan-Thaw et al., where EDS analysis showed the exclusive presence of AuPt alloyed nanoparticles [26]. A high-magnification HAADF STEM image and the corresponding XEDS spectrum from a representative Au_6Pt_4/TiO_2 particle that demonstrates the AuPt alloy structure is shown in Figure S1.

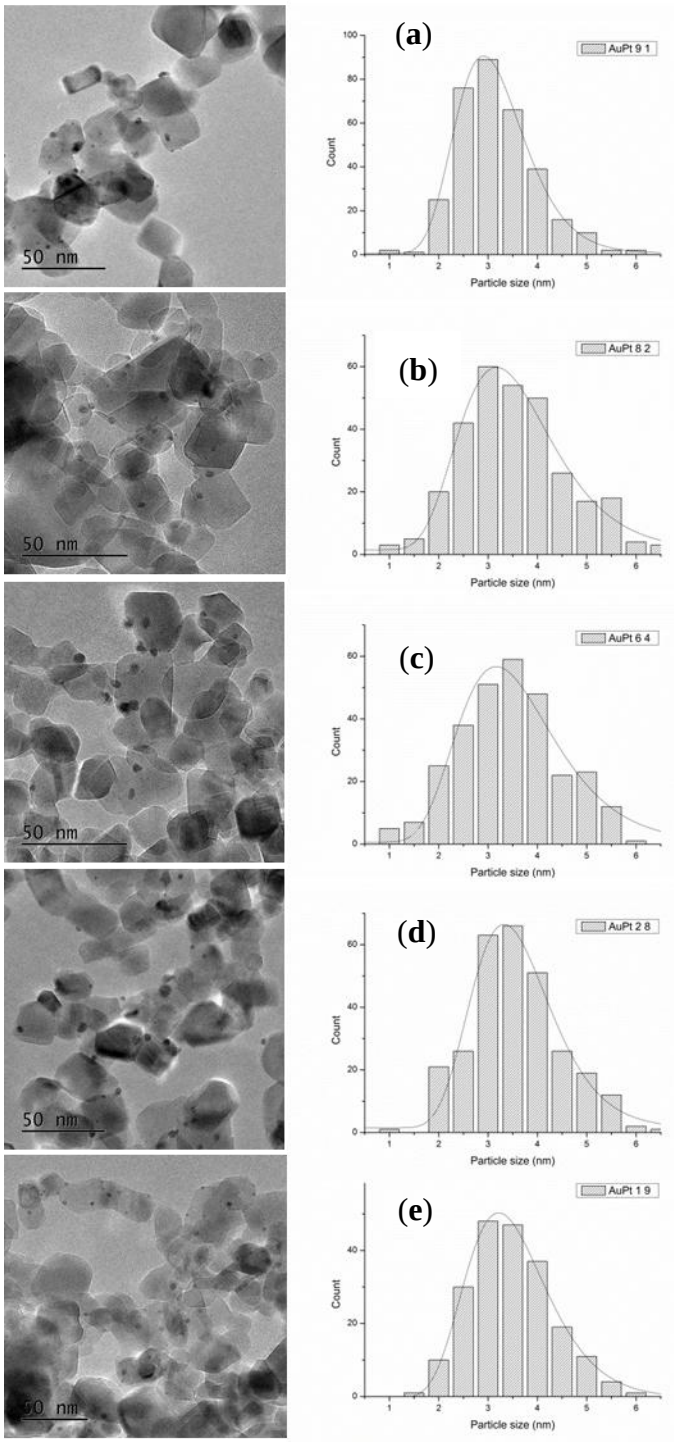

Figure 1. High resolution TEM micrographs (left side and middle) and histogram of particle size distribution (right side) of (**a**) Au_9Pt_1/TiO_2; (**b**) Au_8Pt_2/TiO_2; (**c**) Au_6Pt_4/TiO_2; (**d**) Au_2Pt_8/TiO_2; (**e**) Au_1Pt_9/TiO_2.

To elucidate the oxidation state of the gold and platinum species, XPS was employed (Table 1, Figure S2). The oxidation state of Au at the surface of the catalyst was evaluated by analyzing the values of binding energy (BE) of the $Au4f_{7/2}$ peak. The BE of 83.4 $\pm$ 0.1 eV is evidence that Au is present in the metallic state (Au^0, BE = 84.2 eV). The oxidation state of Pt at the surface of the catalyst was evaluated by analyzing the values of binding energy (BE) of the $Pt4f_{7/2}$ peak. In the bimetallic

samples, the Pt signal presented one species at 70.4 ± 0.2 eV, corresponding to Pt^0. On the contrary the monometallic catalyst presented two contributions, the main one at 71.0 eV corresponding to Pt^0 (77.0%) and a secondary one at 72.4 eV (27.0%) corresponding to Pt^{II} (PtO). The slight decrease to a lower BE than the typical values obtained for metallic gold and platinum (84.0 and 71.4 eV, respectively) could be attributable either to the different degrees of charging of the metal particles in the presence of TiO_2 or to the particle size effect [28–30]. Table 1 shows that BE of Pt4f decreases with an increase of the Au content, being 71.2 eV for monometallic Pt/TiO_2, 70.6 eV for Au_1Pt_9/TiO_2, 70.5 eV for Au_2Pt_8/TiO_2, Au_6Pt_4/TiO_2, Au_8Pt_2/TiO_2 and 70.3 eV for Au_9Pt_1/TiO_2. According to previous reports, these electronic changes in the BE are due to the interaction of Au-Pt due to the formation and presence of AuPt alloy nanoparticles [31,32]. Moreover, the absence of Pt^{II} signal in the bimetallic systems, suggests a strong interaction between Au and Pt which probably prevents the partial oxidation of Pt surface and indicates the presence of gold-rich surface nanoparticles. The AuPt ratio measured by AAS is in good agreement with the nominal one, for almost all the catalysts (Table 1). Moreover, differences are evidenced on the surface atomic composition of the bimetallic nanoparticles measured by XPS. In the case of Au_9Pt_1/TiO_2, Au_6Pt_4/TiO_2, and Au_1Pt_9/TiO_2 catalysts, the Au/Pt atomic ratio measured by XPS is higher by ~30% and in the case of Au_2Pt_8/TiO_2 by 133% than the corresponding bulk Au/Pt atomic ratio, which can indicate surface enrichment of Au atoms in the aforementioned bimetallic nanoparticles (Table 1). On the contrary, Au_8Pt_2/TiO_2, the Au/Pt is lower by ~10% than the corresponding bulk Au/Pt ratio, which can indicate surface segregation of Pt atoms in these nanoparticles.

Table 1. Binding energy of $Au4f_{7/2}$ and $Pt4f_{7/2}$, % abundance of Au and Pt species metal exposure (at %).

Catalyst		Au4f	Pt4f		Au-Pt Atomic Ratio			Au at %	Pt at %	Metal at %
		Au^0	Pt^0	PtO	Nominal	Bulk (AAS)	Surface (XPS)			
1% Au/TiO_2	BE (eV)	83.5	-	-	-	-	-	0.40	-	0.40
	%	100								
1% Au_9Pt_1/TiO_2	BE (eV)	83.3	70.3	-	9.0	9.3	12.0	0.24	0.02	0.26
	%	100	100							
1% Au_8Pt_2/TiO_2	BE (eV)	83.4	70.5	-	4.0	4.2	3.8	0.19	0.05	0.24
	%	100	100							
1% Au_6Pt_4/TiO_2	BE (eV)	83.4	70.5	-	1.5	1.4	1.9	0.14	0.06	0.20
	%	100	100							
1% Au_2Pt_8/TiO_2	BE (eV)	83.4	70.5	-	0.25	0.3	0.7	0.05	0.07	0.12
	%	100	100							
1% Au_1Pt_9/TiO_2	BE (eV)	83.4	70.6	-	0.1	0.1	0.14	0.02	0.14	0.16
	%	100	100							
1% Pt/TiO_2	BE (eV)	-	71.2	72.4	-	-	-	0.02	0.44	0.46
	%		77.0	23.0						

The catalytic performance of the prepared catalysts was evaluated in the liquid phase oxidation of glycerol in the presence of base (NaOH), (Glycerol 0.3 M, Alcohol/metal: 1000, T = 80 °C, pO_2 = 3 atm, 4 eq NaOH) or under base-free conditions (Glycerol 0.3 M, Alcohol/metal: 1000, T = 80 °C, pO_2 = 3 atm) (Table 3 and Figures 2–4). Table 2 reports the activity and selectivity at iso-conversion (90%) in presence of NaOH. The activity was calculated based on the moles of glycerol converted per hour per total mol of metal. All bimetallic systems showed an activity higher (>3000 h^{-1}) than the corresponding monometallic ones (2657 and 2569 h^{-1} for Au/TiO_2 and Pt/TiO_2, respectively) (Table 2 and Figure 2). Considering the bimetallic systems, it can be observed that the best catalytic result was obtained by Au_9Pt_1/TiO_2 (7389 h^{-1}). Decreasing the Au content, the activity progressively decreased, AuPt: 9:1 (7389 h^{-1}) > 8:2 (6845 h^{-1}) > 6:4 (5052 h^{-1}) > 2:8 (3375 h^{-1}) > 1:9 (2569 h^{-1}). Figure 3 shows similar reaction profiles for all the catalysts and no evident deactivation phenomena seem to be present, reaching almost full conversion after 2 h. To confirm the resistance of AuPt catalysts to deactivation,

stability tests have been performed using Au_9Pt_1/TiO_2, the catalyst presenting the highest activity (Table 2). Recycling experiments were carried out by filtering and using the catalyst in the next run without any further purification. The catalyst showed similar conversion and selectivity for six runs (Figure 4). The selectivity of the reaction seems to be strongly influenced by the atomic ratio of Au/Pt. The selectivity has been reported in iso-conversion. It should be noted that the selectivity did not show significant modification as a function of the time on stream (Figure S3). The monometallic Au/TiO_2 catalyst showed a selectivity to glyceric acid of 50%, with glycolic acid (24%) and formic acid (14%), deriving from the C-C cleavage of glyceric acid, as main by-products (Table 2). Increasing the Pt content, a general decrease in the selectivity to glyceric acid was envisaged with the formation of higher amounts of formic and glycolic acid (Table 2). In the case of monometallic Pt/TiO_2, formic acid (40%) was the main product.

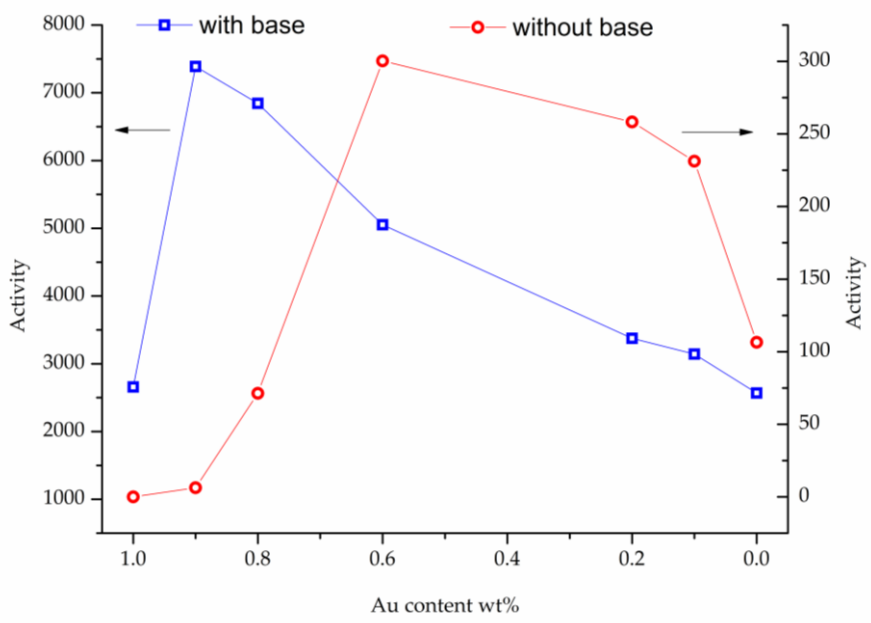

Figure 2. Influence of Au-Pt metal ratio on the initial activity in the glycerol oxidation in presence (blue) and absence (red) of a base.

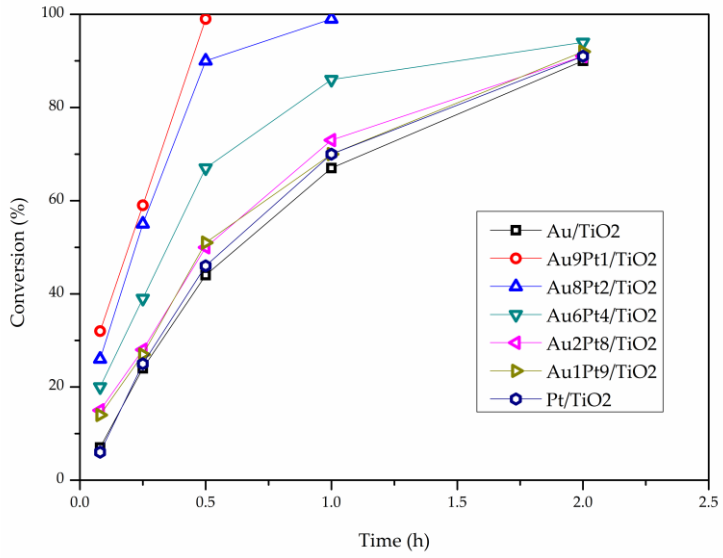

Figure 3. Reaction profile of Au-Pt catalyst in the glycerol oxidation in presence of NaOH.

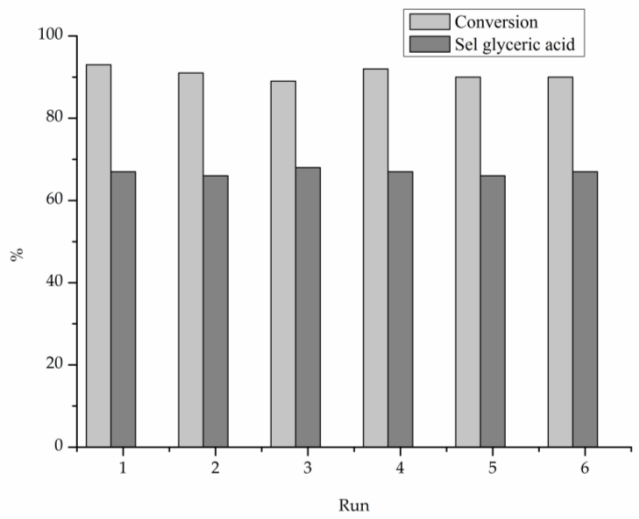

Figure 4. Stability test for Au_9Pt_1/AC in the glycerol oxidation in presence of NaOH, reaction time 0.5 h.

Table 2. Catalytic evaluation in the glycerol oxidation in presence of NaOH [1].

Catalyst	Initial Activity [2]	Selectivity (%) [3]					
		Glyceric Acid	Tartronic Acid	ΣC3 Products	Formic Acid	Glycolic Acid	Oxalic Acid
Au/TiO_2	2657	50	5	55	14	24	4
Au_9Pt_1/TiO_2	7389	58	7	65	10	23	1
Au_8Pt_2/TiO_2	6845	52	7	59	10	28	1
Au_6Pt_4/TiO_2	5052	42	6	48	29	19	1
Au_2Pt_8/TiO_2	3375	36	8	44	33	20	2
Au_1Pt_9/TiO_2	3142	31	6	37	37	16	4
Pt/TiO_2	2569	28	8	36	40	16	5

[1] Reaction conditions. Glycerol 0.3 M, Alcohol/metal: 1000, T = 80 °C, pO_2 = 3 atm, 4 eq NaOH. [2] Mol of alcohol converted per hour per mol of metal, calculated after 0.25 h of reaction. [3] Selectivity calculated at 90% of conversion.

Consecutively, the same series of catalysts were tested in the absence of base (Table 3, Figures 2 and 4). Under base-free conditions Au/TiO_2 was not active, whereas Pt/TiO_2 showed an activity of 112 h^{-1}) (Table 3). For the bimetallic systems, an opposite trend than in the presence of NaOH (Table 2), was observed. Pt-rich bimetallic systems were more active than Au-rich ones, with Au_6Pt_4/TiO_2 showing the most promising catalytic performance, (301 h^{-1}). Au_2Pt_8/TiO_2 and Au_1Pt_9/TiO_2 showed a comparable catalytic activity (263 and 234 h^{-1}, respectively), whereas Au_8Pt_2/TiO_2 and Au_9Pt_1/TiO_2 presented low activity (75 h^{-1} and 7 h^{-1}, respectively).

Table 3. Catalytic evaluation in the base free glycerol oxidation [1].

Catalyst	Initial Activity [2]	Selectivity (%) [3]					
		Glyceric Acid	Glycer-Aldehyde	ΣC3 Products	Formic Acid	Glycolic Acid	Oxalic Acid
Au/TiO_2	-	n.d.	n.d.	n.d.	n.d.	n.d.	n.d.
Au_9Pt_1/TiO_2	7	n.d.	n.d.	n.d.	n.d.	n.d.	n.d.
Au_8Pt_2/TiO_2	75	58	9	67	28	1	n.d.
Au_6Pt_4/TiO_2	301	62	10	72	20	5	n.d.
Au_2Pt_8/TiO_2	263	66	12	88	14	6	n.d.
Au_1Pt_9/TiO_2	234	70	13	83	9	5	1
Pt/TiO_2	112	68	15	83	9	3	2

[1] Reaction conditions. Glycerol 0.3 M, Alcohol/metal: 1000, T = 80 °C, pO_2 = 3 atm. [2] Mol of alcohol converted per hour per mol of metal, calculated after 0.25 h of reaction. [3] Selectivity calculated at 30% of conversion.

Under base-free conditions, the catalyst composition is also influencing the reaction profile (Figure 5). Indeed, Pt-rich AuPt catalyst (Au_2Pt_8/TiO_2) and Pt/TiO_2 monometallic were deactivated after 2 h of reaction, whereas the remaining catalysts showed a higher stability. The stability of AuPt catalysts was further investigated performing recycling tests using Au_6Pt_4/TiO_2 which showed the highest activity (Table 3). The catalyst showed constant conversion and selectivity during the six runs (Figure 6).

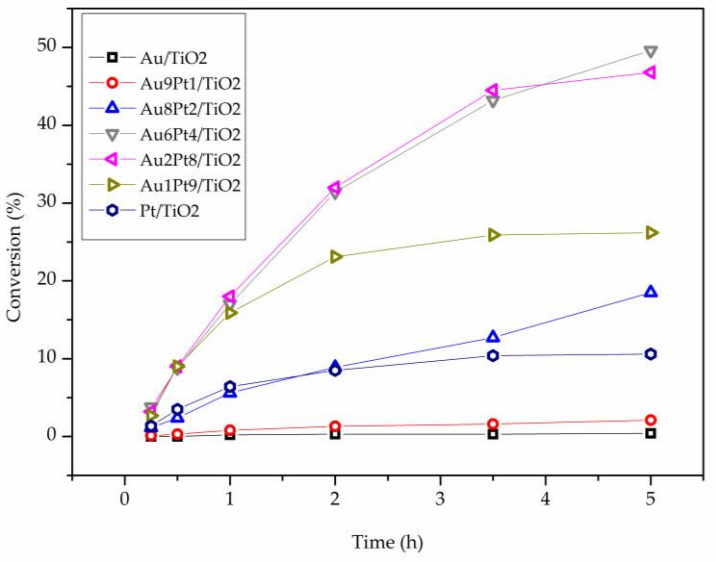

Figure 5. Reaction profile of Au-Pt catalyst in the base free glycerol oxidation.

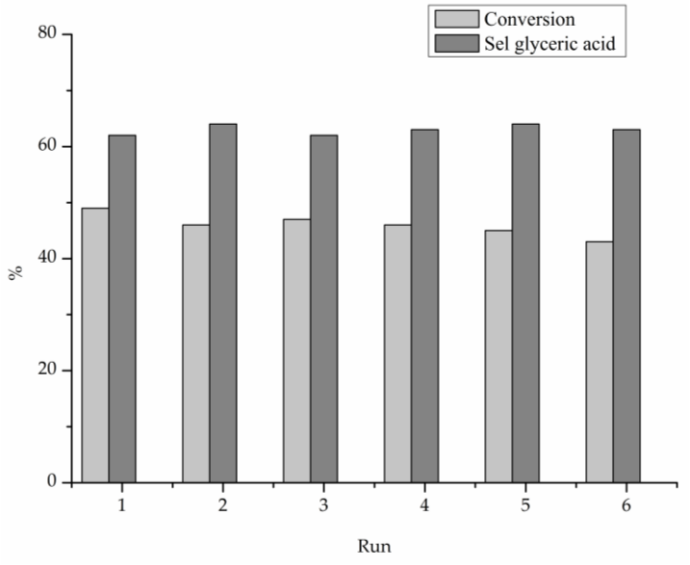

Figure 6. Stability test for Au_6Pt_4/AC in the base free glycerol oxidation, reaction time: 5 h.

In addition, under base-free conditions, glyceric acid was the main product (Table 3). Moreover, glyceraldehyde, which rapidly converts to glyceric acid and base free conditions, was detected. In general, the selectivity to C3 products (67–88%) is higher than using NaOH (42–72%). Correlating the selectivity to Au:Pt atomic ratio, we observed an opposite trend than in the presence of base. Indeed, in this case, Pt-rich systems are more selective to glyceric acid (and glyceraldehyde) than Au-rich ones, with a lower formation of C1 and C2 products deriving from C-C cleavage.

3. Discussion

Au_xPt_y catalysts with different atomic ratios were prepared by sol immobilization with similar mean particle size and narrow particle size distributions as shown by TEM analysis. XPS studies suggest the formation of Au-Pt alloy nanoparticles regardless of the Au_xPt_y atomic composition. The morphology of the catalysts was confirmed by STEM-HAADF and EDS analyses (for Au_6Pt_4/TiO_2). Au_xPt_y catalysts showed different catalytic trends according to the pH of the solution used (presence and absence of base). The whole series of monometallic and bimetallic catalysts showed a lower activity under base -free conditions (initial pH of 4) than in the presence of a strong base (NaOH), despite the higher reaction temperature used (80 °C). This trend was expected as the base has the ability to facilitate the initial step of the reaction and alkoxide formation [33,34] and by favoring the desorption of the highly chelating hydroxyacid, thus, decreasing irreversible adsorption on metal active sites and therefore poisoning [35]. The optimal Au/Pt atomic ratio seems to strongly depend on the pH of the reaction media. In the presence of a strong base, Au_9Pt_1/TiO_2 showed the highest catalytic performance among the series of catalysts studied, whereas under base-free conditions, a higher content of Pt is necessary to achieve the best catalytic activity (Au_6Pt_4/TiO_2). These results are strongly related to the different reaction mechanisms proposed in the case of Au and Pt nanoparticles in the oxidative dehydrogenation. It has been shown that the activation of the O-H group requires a very high activation energy for Au, being lower for Pt [34]. Indeed, Au requires the presence of base to facilitate the first step of the oxidative dehydrogenation, H-abstraction under acid conditions, whereas Pt can carry out this step even under acidic conditions. On the contrary, in the presence of a base, Au-rich catalysts are more active due to the fact that the H-abstraction is favored by the presence of a base. The lower activity of Pt-rich catalysts can be explained by the partial oxidation of Pt surface by molecular oxygen as evidenced during the electrocatalytic oxidation of Au- and Pt-based catalysts [36]. Observing the reaction profiles, deactivation phenomena have been envisaged, in particular in the absence of a base (Figure 4). Under these conditions, Pt-rich catalysts rapidly deactivated, probably due to surface oxidation and chemical poisoning due to the strong chelating properties of the products deriving from glycerol oxidation. According to previous experimental studies, these phenomena are more favored on Pt-rich catalysts than Au-rich ones [37].

In terms of selectivity, an opposite trend was observed according to the pH of the reaction solution. Under base conditions, Au-rich bimetallic catalysts showed higher selectivity to C3 products than Pt-rich ones, which promote the C-C cleavage and the formation of formic and glycolic acid (Table 2). It has been reported that the formation of glycolic and formic acid can be correlated to the generation of H_2O_2, formed through O_2 reduction by the presence of metal hydride [33,38]. Therefore, we determined the amount of H_2O_2 present at the end of the reaction, by titration with $KMnO_4$. For these tests, Au_8Pt_2/TiO_2 and Au_2Pt_2/TiO_2 have been chosen as representing Au-rich and Pt-rich catalysts. Under alkaline conditions, 0.05 mmol/L of H_2O_2 were detected using Au_8Pt_2/TiO_2 whereas 0.44 mmol/L, was detected using Au_2Pt_8/TiO_2, almost a ten times higher amount of H_2O_2. Under acidic conditions, the opposite trend was observed; 0.45 mmol/L of H_2O_2 were detected using Au_8Pt_2/TiO_2 whereas 0.080 mmol/L were detected using Au_2Pt_8/TiO_2. These results are consistent with the selectivity data obtained. To better elucidate the aforementioned experimental results, we performed experiments on the decomposition of H_2O_2 under the following reaction conditions; under alkaline (pH > 14) and 80 °C (Figure 7a) or acidic conditions (pH 4) and 80 °C (Figure 7b) either in the absence or in the presence of Au_8Pt_2/TiO_2 and Au_2Pt_8/TiO_2 catalysts.

Under basic conditions, the degradation of H_2O_2 proceeded fast and no obvious differences between the two catalysts were observed (Figure 5a). Therefore, under basic conditions, probably Pt-rich catalysts promoted to a higher extent the formation of H_2O_2 compared to Au-rich ones favoring the C-C scission, and as a consequence a lower selectivity to C3 products was observed. Under acidic conditions, the decomposition of H_2O_2 is faster on Au_2Pt_8/TiO_2 than on Au_8Pt_2/TiO_2 (Figure 5b), and for this reason, a lower amount of H_2O_2 after reaction was detected and a consequent higher selectivity to glyceric acid was observed for Pt-rich bimetallic systems.

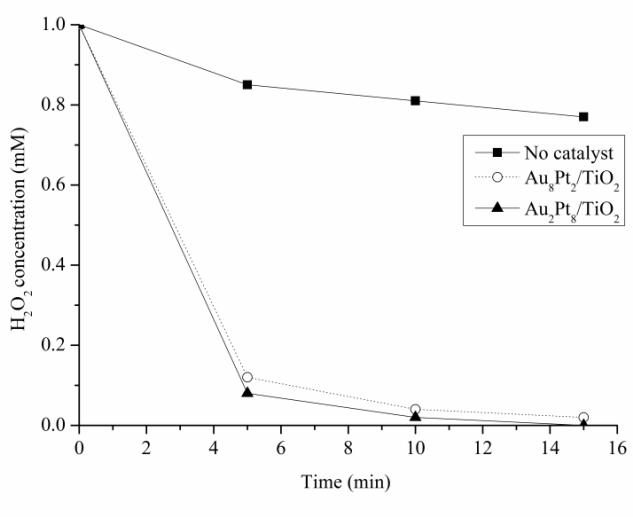

(**a**)

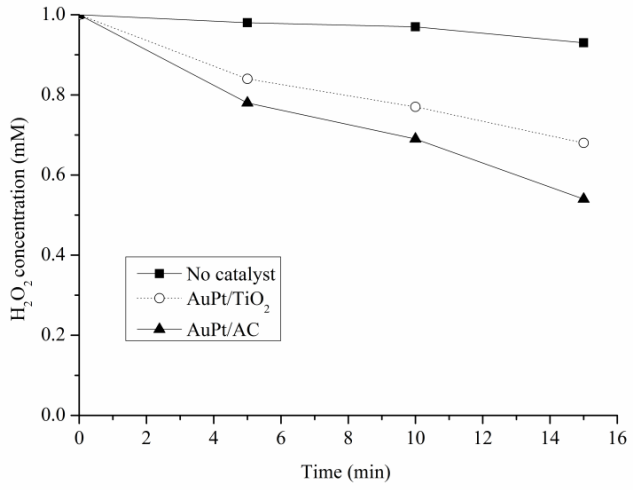

(**b**)

Figure 7. H_2O_2 decomposition at (**a**) 80 °C pH > 14 or (**b**) 80 °C and pH 3.

4. Conclusions

We have studied the catalytic performance of supported AuxPty nanoparticles with different atomic compositions for the glycerol oxidation under base and base-free conditions focusing on the optimization of the Au:Pt atomic ratio to facilitate increase in terms of catalytic performance and improvement in terms of selectivity towards C3 products. The catalysts were synthesized using colloidal-preformed nanoparticles via a well-established sol-immobilization method. The presence of Pt facilitates the increase of the catalytic performance with respect to the Au and Pt monometallic analogues. This could be attributed to the generation of alloyed AuPt nanoparticles in a smaller and narrower particle size range than the Au and Pt monometallic analogues. The most effective catalysts in terms of catalytic activity were with Au:Pt atomic ratio of 6:4 under base-free conditions and Au:Pt atomic ratio of 9:1 under basic conditions showing the importance of alloying Pt with Au. Moreover, stability tests showed the reusability of the alloyed Au_xPt_y catalysts. In terms of selectivity, we found that the formation of C3 products is higher in the absence of base for Pt-rich catalysts than Au-rich catalysts due to the decrease of C-C scission that can be correlated with the presence, concentration and rate of degradation of H_2O_2 under base and base-free conditions.

5. Materials and Methods

5.1. Materials

Glycerol (87 wt % solution), glyceric acid and tartronic acid were purchased from Fluka (Maurice, NJ, USA). $NaAuCl_4 \cdot 2H_2O$, K_2PtCl_4, were from Aldrich (99.99% purity) (St. Louis, MO, USA), TiO_2 (P25) was purchased from Degussa (SA = 50 m^2/g) (Essen, Germany). $NaBH_4$ of purity > 96% from Fluka (Maurice, NJ, USA), polyvinylalcohol (PVA) (Mw = 13,000–23,000 87–89% hydrolysed) from Aldrich (St. Louis, MO, USA) were used. Gaseous oxygen from SIAD was 99.99% pure.

5.2. Catalyst Preparation

Au/TiO_2: Solid $NaAuCl_4 \cdot 2H_2O$ (0.051 mmol) and PVA (1 wt %) solution (Au/PVA = 1/0.5 wt/wt) were added to 100 mL of H_2O. After 5 min, a fresh solution of $NaBH_4$ (0.1 M) ($Au/NaBH_4$ 1/4 mol/mol) was added to the yellow solution under vigorous magnetic stirring. Within a few minutes of sol generation, the colloid was immobilized by adding the support under vigorous stirring. The amount of support was calculated as having a total final metal loading of 1 wt %. After 2 h, the slurry was filtered, the catalyst washed thoroughly with distilled water to remove PVA from the catalyst surface and dried at 80 °C for 4 h.

Pt/TiO_2: Solid K_2PtCl_4 (0.051 mmol) and PVA (1 wt %) solution (Pt/PVA = 1/0.5 wt/wt) were added to 100 mL of H_2O. After 5 min, H_2 was bubbled (50 mL/min) under atmospheric pressure and room temperature for 2 h. The colloid was immobilized by adding the support under vigorous stirring. The amount of support was calculated as having a total final metal loading of 1 wt %. After 2 h the slurry was filtered, the catalyst washed thoroughly with distilled water to remove PVA from the catalyst surface and dried at 80 °C for 4 h.

Au_xPt_y/TiO_2: The preparation of Au_6Pt_4/TiO_2 is reported as an example. $NaAuCl_4 \cdot 2H_2O$ (Au: 0.031 mmol) was dissolved in 60 mL of H_2O, and PVA (1%, wt %) was added (Au/PVA = 1/0.5 wt/wt). The yellow solution was stirred for 3 min, after which a fresh solution of 0.1 M $NaBH_4$ ($Au/NaBH_4$ = 1:4 mol/mol) was added under vigorous magnetic stirring. Within a few minutes of sol generation, the gold sol was immobilized by adding the support under vigorous stirring. The amount of support was calculated as having a gold loading of 0.60 wt %. After 2 h, the slurry was filtered and the catalyst washed thoroughly with distilled water (neutral mother liquors). The Au/support was dispersed in 40 mL of water, with K_2PtCl_4 (Pt: 0.021 mmol) and PVA solution (Pt/PVA = 1:0.5 wt/wt) added. H_2 was bubbled (50 mL/min) under atmospheric pressure and room temperature for 2 h. The slurry was filtered, the catalyst washed thoroughly with distilled water to remove PVA from the catalyst surface and dried at 80 °C for 4 h. The total metal loading was 1 wt %. Using the same procedure and varying the ration between Au and Pt, the following catalysts were prepared: Au_9Pt_1/TiO_2, Au_8Pt_2/TiO_2, Au_6Pt_4/TiO_2, Au_2Pt_8/TiO_2, Au_1Pt_9/TiO_2

5.3. Catalytic Tests

Glycerol oxidation: Catalytic reactions were carried out in a 30 mL glass reactor equipped with a thermostat and an electronically controlled magnetic stirrer connected to a 5000 mL reservoir charged with oxygen (3 atm). The oxygen uptake was followed by a mass-flow controller connected to a PC through an A/D board, plotting a flow time diagram.

Glycerol 0.3 M, and the catalyst (substrate/total metal = 1000 mol/mol) were mixed in distilled water (total volume 10 mL) and 4 equivalents of NaOH. The reactor was pressurized at 3 atm of oxygen and set to 80 °C. In the case of base free glycerol oxidation, Glycerol 0.3 M, and the catalyst (substrate/total metal = 1000 mol/mol) were mixed in distilled water (total volume 10 mL). The reactor was pressurized at 3 atm of oxygen and set to 80 °C. Once the temperature was reached, the gas supply was switched to oxygen and the monitoring of the reaction started. The reaction was initiated by stirring.

Samples were removed periodically and analyzed by high-performance liquid chromatography (HPLC) using a column (Alltech OA- 10,308, 300 mm_7.8 mm) with UV and refractive index (RI) detection to analyze the mixture of the samples. Aqueous H_3PO_4 solution (0.1 wt %) was used as the eluent. Products were identified by comparison with the original samples. Recycling tests were carried out under the same experimental conditions (Glycerol 0.3 M, Alcohol/metal: 1000, T = 80 °C, pO_2 = 3 atm, 4 eq NaOH or Glycerol 0.3 M, Alcohol/metal: 1000, T = 80 °C, pO_2 = 3 atm). The catalyst was recycled in the subsequent run after filtration without any further treatment. Alternatively, the catalyst was regenerated by washing with distilled water before reusing it in the successive run. The recovery of the catalyst was always >98%.

Reaction conditions were optimized and kinetic regime verified varying substrate/metal ratio, glycerol concentration, oxygen pressure, temperature and stirring rate.

5.4. Test for Hydrogen Peroxide Detection and Degradation Test

A 1 mM solution of H_2O_2 (15 mL) was stirred at the appropriate temperature under N_2 atmosphere. The pH of the solution was adjusted by adding H_2SO_4 0.1 M (pH 4) or NaOH 1 M (pH > 14). The amount of the catalyst added was the same as in the glycerol oxidation (about 60 mg). Hydrogen peroxide was quantified by sampling by permanganate titration. The following procedure has been set up: a sample (5 mL) of the filtered reacting solution was titrated with a 0.01 N $KMnO_4$ solution at constant pH of 7.5 $\pm$ 0.1 (by adding concentrated H_2SO_4). The detection limit of H_2O_2 was 0.01 mM.

5.5. Characterization

Particle size distributions and mean particle size were obtained by means of transmission electron microscopy (TEM) using a JEOL JEM 2100 TEM (Akishima, Tokyo, Japan) operating at 200 kV. Samples for examination were prepared by dispersing the catalyst in ethanol. A drop of the suspension was allowed to evaporate on a holey carbon film supported by a 300-mesh copper TEM grid. Samples were subjected to bright field diffraction contrast imaging experiments. Mean particle sizes and particle size distributions were determined by measuring the size of over 200 particles from different selected areas. The mean particle diameter (d_m) was calculated by using the formula $d_m = \Sigma d_i n_i / \Sigma n_i$ where n_i was the number of particles of diameter d_i. The error of the particle size measurement was lower than 5%.

The metal content was checked by Atomic Absorption Spectroscopy (AAS) analysis of the filtrate, on a Perkin Elmer 3100 instrument (Waltham, MA, USA).

X-ray photoelectron spectroscopy (XPS) was performed on a Thermo Scientific K-alpha+ spectrometer. Samples were analyzed using a monochromatic Al X-ray source operating at 72 W (6 mA $\times$ 12 kV), with the signal averaged over an oval-shaped area of approximately 600 $\times$ 400 microns. Data was recorded at pass energies of 150 eV for survey scans and 40 eV for high resolution scan with a 1 eV and 0.1 eV step size respectively. Charge neutralization of the sample was achieved using a combination of both low energy electrons and argon ions (less than 1 eV) which gave a Ti2p 3/2 binding energy of 458.8 eV, correspondent to the value of the commercial titanium dioxide (P25).

All data were analyzed using CasaXPS (v2.3.17 PR1.1) using Scofield sensitivity factors and an energy exponent of -0.6.

Supplementary Materials: The following are available online at http://www.mdpi.com/2073-4344/8/2/54/s1, Figure S1: Representative STEM-HAADF image of Au_6Pt_4/TiO_2 catalyst and the corresponding XEDS spectra obtained from the individual nanoparticle, Figure S2: XPS Spectra for $AuPt/TiO_2$ sample, Figure S3: Selectivity versus time one stream for Au_9Pt_1/TiO_2 in presence of NaOH.

Author Contributions: Andrea Jouve and Alberto Villa designed the experiments and carried out catalytic evaluations; Davide Motta carried out the XPS experiments and helped in the interpretation; Felipe Sanchez Trujillo carried out the TEM and helped in the interpretation; Alberto Villa, Nikolaos Dimitratos and Laura Prati were involved in the writing and editing of the manuscript.

Conflicts of Interest: The authors declare no conflict of interest.

References

1. Corma, A.; Iborra, S.; Velty, A. Chemical routes for the transformation of biomass into chemicals. *Chem. Rev.* **2007**, *107*, 2411–2502. [CrossRef] [PubMed]
2. Okkerse, C.; van Bekkum, H. From fossil to green. *Green Chem.* **1999**, *1*, 107–114. [CrossRef]
3. Behr, A.; Eilting, J.; Irawadi, K.; Leschinski, J.; Lindner, F. Improved utilisation of renewable resources: New important derivatives of glycerol. *Green Chem.* **2008**, *10*, 13–30. [CrossRef]
4. Katryniok, B.; Kimura, H.; Skrzyńska, E.; Girardon, J.-S.; Fongarland, P.; Capron, M.; Ducoulombier, R.; Mimura, N.; Paul, S.; Dumeignil, F. Selective catalytic oxidation of glycerol: Perspectives for high value chemicals. *Green Chem.* **2011**, *13*, 1960–1979. [CrossRef]
5. Kimura, H.; Tsuto, K.; Wakisaka, T.; Kazumi, Y.; Inaya, Y. Selective oxidation of glycerol on a platinum-bismuth catalyst. *Appl. Catal. A Gen.* **1993**, *96*, 217–228. [CrossRef]
6. Garcia, R.; Besson, M.; Gallezot, P. Chemoselective catalytic oxidation of glycerol with air on platinum metals. *Appl. Catal. A Gen.* **1995**, *127*, 165–176. [CrossRef]
7. Villa, A.; Dimitratos, N.; Chan-Thaw, C.E.; Hammond, C.; Prati, L.; Hutchings, G.J. Glycerol Oxidation Using Gold-Containing Catalysts. *Acc. Chem. Res.* **2015**, *48*, 1403–1412. [CrossRef] [PubMed]
8. Carrettin, S.; McMorn, P.; Johnston, P.; Griffin, K.; Hutchings, G.J. Selective oxidation of glycerol to glyceric acid using a gold catalyst in aqueous sodium hydroxide. *Chem. Commun.* **2002**, 696–697. [CrossRef]
9. Porta, F.; Prati, L. Selective oxidation of glycerol to sodium glycerate with gold-on-carbon catalyst: An insight into reaction selectivity. *J. Catal.* **2004**, *224*, 397–403. [CrossRef]
10. Wang, D.; Villa, A.; Porta, F.; Su, D.; Prati, L. Single-phase bimetallic system for the selective oxidation of glycerol to glycerate. *Chem. Commun.* **2006**, 1956–1958. [CrossRef] [PubMed]
11. Dimitratos, N.; Lopez-Sanchez, J.A.; Anthonykutty, J.M.; Brett, G.; Carley, A.F.; Tiruvalam, R.C.; Herzing, A.A.; Kiely, C.J.; Knight, D.W.; Hutchings, G.J. Oxidation of glycerol using gold–palladium alloy-supported nanocrystals. *Phys. Chem. Chem. Phys.* **2009**, *11*, 4952–4961. [CrossRef] [PubMed]
12. Chan-Thaw, C.; Campisi, S.; Wang, D.; Prati, L.; Villa, A. Selective Oxidation of Raw Glycerol Using Supported AuPd Nanoparticles. *Catalysts* **2015**, *5*, 131–144. [CrossRef]
13. Ketchie, W.C.; Murayama, M.; Davis, R.J. Selective oxidation of glycerol over carbon-supported AuPd catalysts. *J. Catal.* **2007**, *250*, 264–273. [CrossRef]
14. Xu, J.; Zhang, H.; Zhao, Y.; Yu, B.; Chen, S.; Li, Y.; Hao, L.; Liu, Z. Selective oxidation of glycerol to lactic acid under acidic conditions using AuPd/TiO_2 catalyst. *Green Chem.* **2013**, *15*, 1520–1525. [CrossRef]
15. Evans, C.D.; Kondrat, S.A.; Smith, P.J.; Manning, T.D.; Miedziak, P.J.; Brett, G.L.; Armstrong, R.D.; Bartley, J.K.; Taylor, S.H.; Rosseinsky, M.J.; et al. The preparation of large surface area lanthanum based perovskite supports for AuPt nanoparticles: Tuning the glycerol oxidation reaction pathway by switching the perovskite B site. *Faraday Discuss.* **2016**, *188*, 427–450. [CrossRef] [PubMed]
16. Wang, D.; Villa, A.; Porta, F.; Prati, L.; Su, D. Bimetallic Gold/Palladium Catalysts: Correlation between Nanostructure and Synergistic Effects. *J. Phys. Chem. C* **2008**, *112*, 8617–8622. [CrossRef]
17. Zhao, Z.; Arentz, J.; Pretzer, L.A.; Limpornpipat, P.; Clomburg, J.M.; Gonzalez, R.; Schweitzer, N.M.; Wu, T.; Miller, J.T.; Wong, M.S. Volcano-shape glycerol oxidation activity of palladium-decorated gold nanoparticles. *Chem. Sci.* **2014**, *5*, 3715–3728. [CrossRef]
18. Villa, A.; Veith, G.M.; Prati, L. Selective Oxidation of Glycerol under Acidic Conditions Using Gold Catalysts. *Angew. Chem. Int. Ed.* **2010**, *49*, 4499–4502. [CrossRef] [PubMed]
19. Brett, G.L.; He, Q.; Hammond, C.; Miedziak, P.J.; Dimitratos, N.; Sankar, M.; Herzing, A.A.; Conte, M.; Lopez-Sanchez, J.A.; Kiely, C.J.; et al. Selective Oxidation of Glycerol by Highly Active Bimetallic Catalysts at Ambient Temperature under Base-Free Conditions. *Angew. Chem. Int. Ed.* **2011**, *50*, 10136–10139. [CrossRef] [PubMed]
20. Rodrigues, E.G.; Pereira, M.F.R.; Chen, X.; Delgado, J.J.; Órfão, J.J.M. Selective Oxidation of Glycerol over Platinum-Based Catalysts Supported on Carbon Nanotubes. *Ind. Eng. Chem. Res.* **2013**, *52*, 17390–17398. [CrossRef]
21. Villa, A.; Campisi, S.; Mohammed, K.M.H.; Dimitratos, N.; Vindigni, F.; Manzoli, M.; Jones, W.; Bowker, M.; Hutchings, G.J.; Prati, L. Tailoring the selectivity of glycerol oxidation by tuning the acid–base properties of Au catalysts. *Catal. Sci. Technol.* **2015**, *5*, 1126–1132. [CrossRef]

22. Tongsakul, D.; Nishimura, S.; Ebitani, K. Platinum/Gold Alloy Nanoparticles-Supported Hydrotalcite Catalyst for Selective Aerobic Oxidation of Polyols in Base-Free Aqueous Solution at Room Temperature. *ACS Catal.* **2013**, *3*, 2199–2207. [CrossRef]
23. Yang, G.-Y.; Shao, S.; Ke, Y.-H.; Liu, C.-L.; Ren, H.-F.; Dong, W.-S. PtAu alloy nanoparticles supported on thermally expanded graphene oxide as a catalyst for the selective oxidation of glycerol. *RSC Adv.* **2015**, *5*, 37112–37118. [CrossRef]
24. Sánchez, B.S.; Gross, M.S.; Querini, C.A. Pt catalysts supported on ion exchange resins for selective glycerol oxidation. Effect of Au incorporation. *Catal. Today* **2017**, *296*, 35–42. [CrossRef]
25. Shen, Y.; Li, Y.; Liu, H. Base-free aerobic oxidation of glycerol on TiO_2-supported bimetallic Au-Pt catalysts. *J. Energy Chem.* **2015**, *24*, 669–673. [CrossRef]
26. Chan-Thaw, C.E.; Chinchilla, L.E.; Campisi, S.; Botton, G.A.; Prati, L.; Dimitratos, N.; Villa, A. AuPt Alloy on TiO_2: A Selective and Durable Catalyst for l-Sorbose Oxidation to 2-Keto-Gulonic Acid. *ChemSusChem* **2015**, *8*, 4189–4194. [CrossRef] [PubMed]
27. Villa, A.; Manzoli, M.; Vindigni, F.; Chinchilla, L.E.; Botton, G.A.; Prati, L. Diols Production From Glycerol Over Pt-Based Catalysts: On the Role Played by the Acid Sites of the Support. *Catal. Lett.* **2017**, *147*, 2523–2533. [CrossRef]
28. Radnik, J.; Mohr, C.; Claus, P. On the origin of binding energy shifts of core levels of supported gold nanoparticles and dependence of pretreatment and material synthesis. *Phys. Chem. Chem. Phys.* **2003**, *5*, 172–177. [CrossRef]
29. Arrii, S.; Morfin, F.; Renouprez, A.J.; Rousset, J.L. Oxidation of CO on Gold Supported Catalysts Prepared by Laser Vaporization: Direct Evidence of Support Contribution. *J. Am. Chem. Soc.* **2004**, *126*, 1199–1205. [CrossRef] [PubMed]
30. Zwijnenburg, A.; Goossens, A.; Sloof, W.G.; Crajé, M.W.J.; Van der Kraan, A.M.; De Jongh, L.J.; Makkee, M.; Moulijn, J.A. XPS and Mössbauer characterization of Au/TiO_2 propene epoxidation catalysts. *J. Phys. Chem. B* **2002**, *106*, 9853–9862. [CrossRef]
31. Yung, T.-Y.; Liu, T.-Y.; Huang, L.-Y.; Wang, K.-S.; Tzou, H.-M.; Chen, P.-T.; Chao, C.-Y.; Liu, L.-K. Characterization of Au and Bimetallic PtAu Nanoparticles on PDDA-Graphene Sheets as Electrocatalysts for Formic Acid Oxidation. *Nanoscale Res. Lett.* **2015**, *10*, 365. [CrossRef] [PubMed]
32. Park, H.-Y.; Jeon, T.-Y.; Jang, J.H.; Yoo, S.J.; Choi, K.-H.; Jung, N.; Chung, Y.-H.; Ahn, M.; Cho, Y.-H.; Lee, K.-S.; et al. Enhancement of oxygen reduction reaction on PtAu nanoparticles via CO induced surface Pt enrichment. *Appl. Catal. B Environ.* **2013**, *129*, 375–381. [CrossRef]
33. Ketchie, W.C.; Fang, Y.-L.; Wong, M.S.; Murayama, M.; Davis, R.J. Influence of gold particle size on the aqueous-phase oxidation of carbon monoxide and glycerol. *J. Catal.* **2007**, *250*, 94–101. [CrossRef]
34. Zope, B.N.; Hibbitts, D.D.; Neurock, M.; Davis, R.J. Reactivity of the Gold/Water Interface during Selective Oxidation Catalysis. *Science* **2010**, *330*, 74–78. [CrossRef] [PubMed]
35. Dimitratos, N.; Villa, A.; Wang, D.; Porta, F.; Su, D.; Prati, L. Pd and Pt catalysts modified by alloying with Au in the selective oxidation of alcohols. *J. Catal.* **2006**, *244*, 113–121. [CrossRef]
36. Kwon, Y.; Schouten, K.J.P.; Koper, M.T.M. Mechanism of the Catalytic Oxidation of Glycerol on Polycrystalline Gold and Platinum Electrodes. *ChemCatChem* **2011**, *3*, 1176–1185. [CrossRef]
37. Zope, B.N.; Davis, R.J. Inhibition of gold and platinum catalysts by reactive intermediates produced in the selective oxidation of alcohols in liquid water. *Green Chem.* **2011**, *13*, 3484–3491. [CrossRef]
38. Prati, L.; Spontoni, P.; Gaiassi, A. From Renewable to Fine Chemicals Through Selective Oxidation: The Case of Glycerol. *Top. Catal.* **2009**, *52*, 288–296. [CrossRef]